# Title:

The Computational Neuroanatomy of Predictive Dynamics of Pain Perception

## Author names and affiliations

Ryota Ishikawa [1] and *Jun Izawa [2]

[1]Ph.D. Program in Humanics, University of Tsukuba, Ibaraki 305-8573, Japan

[2]Faculty of Engineering, Information, and Systems, University of Tsukuba, Ibaraki 305-8573, Japan

*Corresponding author:

Jun Izawa

Faculty of Engineering, Information, and Systems

University of Tsukuba

1-1-1 Tennodai, Tsukuba, Ibaraki 305-8573, Japan

Tel.: +81-29-853-3756; Email: izawa@emp.tsukuba.ac.jp

## Abstract

Pain perception is an active process that regulates nociceptive inputs by descending opioidergic signals, in which the brain encodes pain-related predictive and corrective terms, after having made Bayesian-like inferences about noxious amplitudes. Offset analgesia (OA), a large reduction of tonic pain after a small nociceptive termination, is typical empirical evidence of on-line pain modulation through prediction and its correction. However, the basic computational structure underlying OA is not understood. Here, we adopted a constructive approach, formulated the inference of noxious amplitudes with a Kalman filter model, i.e., a recursive Bayesian computation, and then deduced the computational structure for OA, in which an interaction between two latent state variables was implemented. Simulation results suggested that the unidirectional interaction of the two states with two dissociable roles (an integral over time and a derivative of stimulus changes) is crucial for OA. Our results, combined with previous anatomical studies, suggest a computational basis of neural connectivity for pain. The ACC and aINS interact to compute a descending prediction to the brainstem, i.e. PAG, while ascending inputs are filtered in the thalamus and delivered to the cortices as prediction errors. Thus, we suggest dissociable, computational roles of the ACC and aINS in pain processing.


## Author Summary

Understanding the computational theory of pain perception is crucial for clarifying why some painful syndromes become chronic. Here, we propose a computational neuroanatomical model of endogenous pain modulation and we simulate a model for offset analgesia. We first demonstrate through model comparisons that the brain encodes at least two distinct states to estimate ongoing nociception: a derivative of input changes and its integral. We suggest that its neural substrate comprises hierarchical circuits composed of cortices, the thalamus, and brainstem. Second, we show that the computational basis of disrupted pain modulation in patients is pseudo-neglect of actual sensory inputs, with bias toward the internal prediction. Our results are the first to provide

41 a neurocomputational mechanism of pain perception dynamics and a factor that determines its
42 functionality.

43

# Introduction

Pain processing is an essential cognitive function for organismal survival. After an injury, persisting tonic pain is an important cue to monitor the condition of the body and to choose appropriate actions, e.g., resting, favoring the injured structure, or escaping. Modern theories have proposed that multiple regions and the network they form (Fig. 1) represent such pain processing [1–3], since there is no unitary region for pain in the brain, i.e., a "pain cortex"[4–6]. However, because of its complexity, the means by which the neural processing of these regions is integrated still remains puzzling.

**Fig.1 | A consensus on neuroanatomy and a pain processing network.** The representative theory of the neural mechanism of pain postulates ascending and descending pathways [3,35–37]. The ascending pathway (red arrows) conveys nociceptive inputs from the spinal cord to the cortex via the thalamic nucleus. The descending pathway projects from cortical regions to the brainstem, e.g., the Periaqueductal Gray (PAG) or the Rostral Ventromedial Medulla (RVM), finally arriving at the spinal cord to modulate further afferent inputs (black arrows). It has been thought that in this process there should be two modulatory circuits, i.e., one that consists of the anterior cingulate cortex (ACC) and the prefrontal cortex (PFC), which provide emotional modulation (green dashed arrow), and another that consists of the anterior insula cortex (aINS) and the amygdala (AMY), which supply attentional modulation (cyan solid arrow).

Theoretically, Bayesian computation is fundamental in sensory perception, such as vision and touch [7–11]. Pain perception is also thought to involve Bayesian computation. For instance, various studies have suggested that placebo and nocebo effects for phasic pain, e.g., a pulse of noxious heat, can be explained by Bayesian inference of pain, in which the prediction of nociceptive inputs, i.e., priors, is integrated with the stimulus input, i.e., likelihood, leading to

pain perception, i.e., posterior [12–16]. Meanwhile, the current painful experience itself should provide effective cues to expect incoming tonic pain. For example, an increase in pain intensity often signals still more pain to come [17].

Offset analgesia (OA) is well-known empirical evidence of this effect, defined as a disproportionately large reduction of perceived pain intensity immediately after a small, i.e., 1℃ decrease in the presented temperature [18–20]. Hyperalgesia, which is induced by the opposite temperature pattern of OA is called onset hyperalgesia (OH), and is thought to have a common neural basis, although there is less empirical and neuroimaging evidence [21–23]. Since these temporal dynamics characterize neural processing tonic pain, illustrating the computational model based on Bayesian inference should be useful to ascertain which neural structures are engaged and how they contribute.

Clinically, OA has been used as an index of endogenous pain modulation, and the deficit of this phenomenon, i.e., less or no analgesic effect after reduction of a noxious heat stimulus, has been reported in patients with neuropathic pain [24,25] and other chronic pain syndromes [26–30]. These dysfunctions can be caused by descending modulatory regions, e.g., the anterior cingulate cortex (ACC) and brainstem, which showed weaker BOLD signals in patients than in healthy controls [31]. This seemed to produce a slower pain perception [28], but few investigations have identified the neuropathological mechanism underlying attenuation of OA in chronic pain patients [32].

To figure out the computational structure underlying OA and OH, we have built a computational model of tonic pain perception, based on a recursive Bayesian computational process, i.e., a Kalman filter [33]. The purpose here is to test various structures of hidden causes of pain, i.e., latent states and noxious intensity, i.e., observable value, in Kalman filter models that are necessary to replicate characteristics of OA and OH reported in human studies (Fig. 2). This approach to computational structure may also reveal corresponding neural structures with dissociable cortical functions [34]. In particular, the total number of hidden variables and how

they interact in the identified computational model, provide a basis to understand how many neural areas are involved and how they are connected in the brain. For example, it is widely known that emotion and attention are processed in distinct descending circuits to modulate pain [3,35–37] (Fig. 1) . This can be modeled by the two latent states that interact equivalently, or else there is no interaction between them. Meanwhile, the predictive coding framework [38–40] has proposed a hierarchical structure between neural populations to encode the world, i.e., top-down predictive pathways and bottom-up corrective pathways.

**Fig.2 | Offset analgesia and onset hyperalgesia. (A)** The pain intensity rating for the temperature of the offset analgesia (OA) condition (solid red line) showed an increase in T2, but was largely reduced in T3 compared to the constant condition (dashed black line). **(B)** The pain intensity rating for the temperature of the onset hyperalgesia (OH) condition (solid cyan line) decreased in T2, but largely increased in T3 compared to the constant condition (dashed black line). **(C)** Removing the effect of habituation, which resulted in a gradual rating decrease over time in all conditions, deviations of the pain intensity rating of OA and OH from that of the constant condition revealed more clearly the OA and OH phenomena. These temperature patterns and pain intensity ratings were reproduced in accordance with previous literature[22].

Thus, we hypothesized that the brain represents one or more latent state variables that represent an environmental source of pain and that this computational structure is crucial for OA and OH. (1) In order to explain OA and OH, are two latent states necessary or not? (2) If so, how do they generate observable output? (3) How do they interact? (4) How does this theory explain the neural basis of chronic pain? By identifying these structures in a framework of predictive coding with the normative model using Kalman filter theory, we provide insights on the unknown anatomical structure involved in tonic pain processing as a computational constraint on neuroanatomy.

# Results

*General framework*

Typical temporal profiles of OA and OH are shown in Figs. 2A-B. During T3 phase, on-line rating of perceived pain intensity was undershot in the OA condition and overshot in the OH condition, compared to the constant baseline condition (Fig. 2C). Here, we aimed to replicate such effects with our computational models. Our model, based on a Kalman filter, comprises two processes: state prediction and state estimation. In the state prediction phase, the latent state in the next time step is predicted by the previous estimate. In the state estimation phase, such a prediction is refined by prediction error, i.e., the difference between measured input and its estimate after filtering, depending on measurement precision.

We test our computational models and examine which structure may explain the properties of human pain perception with the representative experiment paradigm that uses the continuous heat stimuli on the skin, including a slight decrease and increase above the pain threshold (Fig. 3A). The thermal stimulus consisted of three phases: the initial painful stimulus (T1, during 5 sec), 1-2℃ increase/decrease to the second stimulus (T2, during 5 sec), and return to the T1 stimulus (T3, during 10 sec). In T3 phase, perceived pain intensity is expected to reduce/increase disproportionately to the presented temperature. Compared to the baseline condition (T1:45-T2:45-T3:45℃, BL), we tested two temperature patterns of (1) OA1: 45-46-45℃ and (2) OA2: 45-47-45℃. The OA2 condition should be useful for testing whether the extent of the analgesic effect is proportional to the step size [23], i.e., the step size of +2℃ results in a larger analgesic effect than that of +1℃. Furthermore, to account for a bidirectional modulation, i.e., OH, in a unified model, we also decided to test the OH1 condition, (3) OH1: 45-44-45℃, where the perceived pain intensity is expected to increase disproportionately in T3 phase. All of these four stimulus patterns start from 44.5℃ (1sec) and terminate with 44℃ (1sec), which is just above the pain threshold, since OA and OH have been discussed as phenomena for painful stimuli, not painless ones.

**Fig.3 | Thermal stimulus and single-state model. (A)** The thermal stimulus used in the simulations. **(B)** Diagram of single-state model structure. The circle indicates the latent variable, and the square indicates the measurement estimate. The magenta arrow indicates the prediction of the next state. The blue arrow indicates the measurement estimate from the predicted latent variable. The state equation and measurement equation are described within the gray rectangle. **(C)** The left is the simulation result of pain intensity. Simulations under the conditions of four temperature patterns are shown by dotted black, solid red, green, and cyan lines. The black arrow indicates that the single-state model did not induce any effects of OA or OH. The right is the simulation result of a latent state variable under the OA2 condition. The dotted green line indicates the dynamics of the latent variable, and the solid black line indicates the temperature pattern of OA2.

*The single state did not explain OA or OH.*

We first tested whether the single-state model (Fig. 3B) could replicate OA and OH. The main goals of this simulation were to determine: (1) whether OA1/OA2 conditions produce an undershoot, i.e., analgesia, in T3 phase and (2) whether the OH1 condition produces an overshoot, i.e., hyperalgesia in T3 phase. Briefly, this model failed to produce these phenomena, since there were no undershoots/overshoots in T3 phase. (Fig. 3C, left). For example, in the OA2 condition, the latent state variable of the pain prediction $\hat{x}$ increased in T2 phase, but in T3 phase diminished to the same value as in T1 phase, without any deviation from the presented temperature (Fig, 3C, right). This indicated that although the Kalman filter model with the single state successfully estimated the presented temperature accurately, it did not replicate either OA or OH. These results suggest that more than one state variable in the Kalman filtering model is necessary to reproduce OA and OH phenomena. Results of further model testing with two-state models are shown in the

following sections.

*Model comparison within model family 1: the parallel contribution of the state to measurement estimation.*

In model family 1, where two state variables ($\hat{x}_1$, $\hat{x}_2$) additively generate a prediction of pain intensity, we tested three model structures. The graphical models and corresponding state-space representations of the tested models are summarized in Fig. 4A. In the "No interaction" model (Nint), $\hat{x}_1$ and $\hat{x}_2$ do not interact, i.e., each of them is predicted independently in the next step from its own previous estimate. In the "Unidirectional interaction" model (Uint), $\hat{x}_1$ in the next step is updated from both previous estimates of $\hat{x}_1$ and $\hat{x}_2$, whereas $\hat{x}_2$ in the next step is updated only on its own. In the "Bidirectional interaction" model (Bint), both variables in the next step are predicted from their own and the other's previous estimates.

**Fig.4 | Model family 1.** (**A**) Diagrams of each model structure. Circles indicate latent variables, and squares indicate the measurement estimate. Magenta arrows indicate the prediction of the next state. Blue arrows indicate the measurement estimate from latent variables. The state and measurement equations are described in the gray rectangles. (**B**) Simulation results of pain intensity under four temperature patterns are shown by dotted black, solid red, green, and cyan lines. **(C)** Simulation results of latent state variables in the OA2 condition are depicted by green dashed and dotted lines.

Fig. 4B showed the simulation results for respective stimulus patterns. In all models, estimated pain intensity increased from T1 to T2 in the OA1 condition, following the actual stimulus dynamics. From T2 to T3, however, only the Uint model resulted in an undershoot,

196 relative to constant conditions, i.e., OA, whereas the other two models showed no such effect.
197 The analgesic effect in the Uint model was larger in OA2 than OA1, which was consistent with
198 literature indicating that the degree of analgesia depends on the shift size [23]. Furthermore, in
199 the OH1 condition, only the Uint model showed an overshoot in T3, i.e., OH. The Bint model
200 resulted in enlarged peaks, but showed no undershoot/overshoot.

201 These results may be caused by differences in temporal profiles of the evolution of two
202 latent state variables (Fig. 4C). In particular, it should be noted of the Uint model, that the
203 temporal profiles of $\hat{x}_1$ and $\hat{x}_2$ were significantly dissociable, as if they have different roles. $\hat{x}_1$
204 slowly tracked the abrupt change of the stimulus, whereas $\hat{x}_2$ quickly responded to the abrupt
205 change, but did not sustain its value when the stimulus became constant. In other words, $\hat{x}_1$
206 represents an integral over time and $\hat{x}_2$ represents a derivative of a stimulus change. Our
207 simulation suggests that the unidirectional interaction between the two variables characterizes
208 two different roles of latent variables, which are necessary to replicate OA/OH phenomenon.
209 This further suggests that these differences in the functional roles of two state variables may
210 characterize the different temporal dynamics of neural activities associated with the
211 representations of two state variables.

212

213 *Model comparison within model family 2: the solitary contribution of the state-to-measurement*
214 *estimate.*
215 In model family 2, where only one of the two state variables ($\hat{x}_1$) generates pain intensity, we
216 also tested three model structures. The graphical models and corresponding state-space
217 representations of the tested models are summarized in Fig. 5A. Two of these *A* matrices are
218 shared with those in model family 1, except $A_{IUint}$. In the "Unidirectional interaction" model
219 (Uint), a latent variable $\hat{x}_1$, which predicts the next state from previous estimates of both $\hat{x}_1$ and

220 $\hat{x}_2$, is used to estimate the measurement. In the "Inverted Unidirectional interaction" model
221 (IUint), on the other hand, a latent variable $\hat{x}_1$, which predicts the next state from only its own
222 previous estimate, is used to estimate the measurement, and the other state $\hat{x}_2$ is updated by the
223 previous estimate of both $\hat{x}_1$ and $\hat{x}_2$ but did not directly influence the pain intensity estimate.
224
225 **Fig.5 | Model family 2.** (**A**) Diagrams of each model structure. Circles indicate latent variables,
226 and squares indicate the measurement estimate. Magenta arrows indicate the prediction of the
227 next state. Blue arrows indicate the measurement estimate from latent variables. State dynamics
228 and the measurement equation are described in the gray rectangles. (**B**) Simulation results of
229 pain intensity under four temperature patterns are shown by dotted black, solid red, green, and
230 cyan lines. **(C)** Simulation results of latent state variables in the OA2 condition are depicted by
231 green dashed and dotted lines.
232

233 Simulation results of pain intensity in all conditions and latent variables in the OA2
234 condition are depicted in Fig. 5B and 5C, respectively. As in the result of model family 1, only
235 the Uint model replicated an undershoot/overshoot in T3 phase, while the other models did not.
236 The latent state variables of the Uint model showed the time constant difference, although those
237 of the Bint were identical. One latent variable of IUint, $\hat{x}_2$, diverged from 0, although the pain
238 intensity was similar to that of the Nint model of model family 1. As in the result of model
239 family 1, the temporal profile of $\hat{x}_1$and $\hat{x}_2$ in the Uint model are dissociable, as if $\hat{x}_1$ represents
240 an integral over time and $\hat{x}_2$ represents a derivative of stimulus change. In principle, we did not
241 find a crucial difference in the Uint models between model family 1 and 2, i.e., $H = [1 \quad 1]$ vs.
242 $[1 \quad 0]$.
243

*Aberrant transition noise induces OA dysfunction.*

Given the previous considerations on computational backgrounds of psychiatric disorders (e.g., schizophrenia)[41–44], we hypothesized that chronic pain could be due to too strong prior information compared to the prediction error. To test this, using the Uint model in model family 2, we examined the impact of the variances of transition noise in the OA2 condition by manipulating the transition noise, i.e., prior uncertainty of pain, such that $\sigma_1^2 = \sigma_2^2 = 0.1, 0.03, 0.01,$ or $0.005$. Simulation results of pain intensity with different variances are depicted in Fig. 6A. Smaller variances showed insensitive responses to the temperature increment in T1. They reached the same peak in T2 phase, but their latency was longer, which was consistent with features of chronic pain patients [28]. Notably, models with smaller variances showed less or no undershoot in T3 phase, i.e., small analgesic effects, depicted in a rectangular window in Fig. 6A. This was caused by a difference of Kalman gain, which is calculated as a relative value between transition noise (prior uncertainty) and measurement noise (sensory uncertainty). In fact, smaller variance of transition noise resulted in smaller Kalman gain for either $\hat{x}_1$ or $\hat{x}_2$ (Fig. 6B). Since Kalman gain determines the influence of prediction error on updating the estimate of latent state variables, i.e., smaller Kalman gain ignored the abrupt change in stimulus intensity in T3 phase, measurement estimate maintained high intensity and showed no undershoots. This suggests that such strict sensory filtering and exaggerated dependency on internal prediction of pain resulted in insensitivity to stimulus changes, underlying dysfunction of endogenous pain modulation, like OA, in chronic pain patients [24–31].

**Fig.6 | Impact of variances of transition noise.** **(A)** Simulation results of pain intensity with four variances of transition noise are shown in solid-colored lines. **(B)** Simulation results of Kalman gain of $\hat{x}_1$ (top) and of $\hat{x}_2$ (bottom) with four variances of transition noise are shown in solid-colored lines.

# Discussion

To illustrate the neural mechanism underpinning the active, dynamic process of tonic pain perception, i.e., offset analgesia (OA) and onset hyperalgesia (OH), we investigated the nature of an essential structure of the computational mechanism behind this process. Given that pain perception relies on Bayesian inference [12–16], our working hypothesis is that tonic pain perception can be modeled using a Kalman filter model. First, we showed that the single-state model failed to replicate OA and OH, whereas the supportive models of two states indicated a core feature of model structure necessary to produce OA and OH. There was no difference between the structures of measurement matrix $H$, i.e., $\hat{x}_1$ had to contribute to estimating measurement $\hat{y}$, although the contribution of $\hat{x}_2$ was not always necessary. The state transition matrix $A$ determined a unidirectional interaction of latent variables, i.e., $\hat{x}_1$ in the next step is predicted from $\hat{x}_2$ as well as by $\hat{x}_1$. In this structure, $\hat{x}_1$ and $\hat{x}_2$ showed distinct temporal dynamics, as if $\hat{x}_1$ represents an integral over time and $\hat{x}_2$ represents a derivative of stimulus change. Finally, we suggested that a strong prior belief in pain may cause OA dysfunction in chronic pain patients. These identified computational structures provide insight into the neuroanatomical structure of pain processing.

Which brain regions regulate pain has been a long-standing question in brain science, and pain researchers have focused on the PAG as a key terminal of descending modulatory circuits from the cortex [19,45–49], including offset analgesia [50]. However, cortico-brainstem connectivity has remained intractable because neuroimaging the brainstem requires high-resolution fMRI [45]. At the same time, cortical connectivity relevant to pain processing has been too complicated to understand. In fact, both the ACC [45,51,52] and the aINS [19,53] have descending projections to the PAG, which have been considered crucial to pain modulation, but their functional dissociation still remains unclear (Fig. 1). Here, we approached these questions by formulating the role of the PAG as the prediction of pain intensity ($\hat{y}$). This is because the

BOLD signals of the PAG represented the expectation of pain intensity rather than the actual intensity [54]. If so, the spinal cord should represent the prediction error $y - \hat{y}$, based on the descending prediction $\hat{y}$ and the ascending input $y$ (Fig. 7). This is reasonable since, at the level of spinal cord, decreased neural activity was reported during some kinds of analgesic effect, compared to no modulatory conditions [55,56]. Furthermore, the neural function of the cortical regions, i.e., the aINS and the ACC, should be formulated as estimates of latent state variables $\hat{x}_1$ and $\hat{x}_2$, respectively. Predictive coding seems valid for the pain system [16,17,57,58], and neuroimaging studies indicate that BOLD signals in the aINS and the ACC are explained well by the mixture of prediction and its error, rather than sensory intensity itself [54]. Because our Kalman filter model explicitly formulated prediction and corrective terms using latent state variables, the state interactions described in the transition matrix $A$ imply the basic anatomical structure in the brain, at least in cortical regions, in which neural activity is consistent with the predictive coding framework.

**Fig.7 | Specified neural structures supported by model simulations of OA/OH**. The complicated network, including the brainstem and multiple cortical regions, i.e., ascending and descending pathways of the pain system, is organized in a framework of predictive coding with the Kalman filter model. Signals representing prediction error (red arrows) originate in superficial pyramidal cells (red triangles) and terminate in deep pyramidal cells (black triangles), traveling from lower regions to higher regions. Conversely, signals representing predictions (black arrows) originate in deep pyramidal cells and terminate in superficial pyramidal cells, traveling from higher to lower regions. The blue triangle indicates matrix cells, that encode information about the precision of the prediction error and control relative influences on prediction updates.

By modeling cortico-brainstem connectivity as the structure of the measurement matrix $H$, we can tackle a question on the neural mechanism of pain processing: What is the structure of the descending circuit to the PAG from the cortex? We found that the structure of $H$ might take two possible forms. One is that both latent variables, $\hat{x}_1$ and $\hat{x}_2$, estimate the measurement in parallel, i.e., $H = [1 \quad 1]$, as in model family 1. The other is that only one latent variable $\hat{x}_1$ has to contribute to the estimate of measurement, i.e., $H = [1 \quad 0]$, as in model family 2. We did not find a clear difference between the two structures. Previous studies supported the parallel projection on distinct dual modulation systems with the emotional and attentional circuits [3,59] (Fig. 1). In these previous studies, the aINS and the ACC were thought to be involved in the attentional and emotional circuits, respectively. Nevertheless, this theory conflicts with the fact that the ACC also has a crucial role in attentional analgesia [45,60]. How should we interpret the function of these regions and their connectivity in OA and OH? Because of the time course difference of BOLD signals (we will explain in the following section), $\hat{x}_1$ is encoded in the aINS, whereas $\hat{x}_2$ is encoded in the ACC. If so, our results strongly suggested that the descending projection of the aINS to the PAG is a core structure of the general pain modulatory system, while a direct projection of the ACC to the PAG also exists. This is consistent with the aforementioned literature. Moreover, it emphasizes the importance of cortical processing, which determines the amount of pain that is to be modulated [57].

We showed that in both model families, a specific structure of the matrix $A$, i.e., unidirectional interaction from $\hat{x}_2$ to $\hat{x}_1$, replicated OA and OH phenomena. This structure provided these two variables with different roles, as if $\hat{x}_1$ served as an integral over time, whereas $\hat{x}_2$ served as a derivative of the stimulus change. This conclusion, derived from the examination of computational structure, provides a constraint on possible functional connectivity between cortical regions engaged in tonic pain processing. One such region is the ACC, which in fact, activated even before stimulus onset, i.e., during expectation or anticipation [47,51,52,61,62].

345 Furthermore, the ACC was more activated when less controllability was perceived over
346 nociception [63,64], where a large prediction error should occur. This neural implementation is
347 called predictive coding, and another cortical region that shows similar neural activation for pain
348 processing is the aINS[53,54,65,66]. Their connectivity has been considered a cortical center of
349 fine-tuned pain regulation [18,67–70], although their functional roles have seemed
350 indistinguishable. Our results provide an explanation for this paradox: the aINS represents the
351 integral term of noxious stimuli ($\hat{x}_1$), whereas the ACC represents a derivative term ($\hat{x}_2$). This
352 dissociation is consistent with the time course difference of BOLD signals observed during tonic
353 pain processing, in which the onset of activation of the ACC was early compared to that of the
354 aINS, while the response duration of the ACC is shorter than that of the aINS [64,71]. Such
355 differences could originate from the unidirectional connectivity, which could implement
356 messages passing from the higher state in the ACC to the lower state in the aINS about the cause
357 of nociception.

358 The current models calculated the Kalman gain based on the measurement and
359 transition noise, which together, control the impact of the prediction error ($y - \hat{y}$) to update the
360 state prediction. In addition, we showed that smaller variances of transition noise resulted in
361 smaller Kalman gain, reducing sensitivity and disrupting OA effects. Thus, this theory explains
362 that disrupted OA in chronic pain patients [24–31] is caused by abnormal filtering due to
363 excessive dependence on top-down pain predictions rather than bottom-up signals. Such a gain
364 control, depending on the precision of the signal, is necessary for the brain to attend precise
365 information more than a noisy one. For example, a noisy retinal input, e.g., a visual stimulus
366 distracted by something, is ignored in the visual system, whereas a precise one, e.g., an attended
367 visual stimulus, is assimilated in the higher visual cortex [72]. This process is implemented in
368 one of the nuclei in the thalamus pulvinar [72,73]. Then, which region performs such a gain
369 control function in the pain system? The thalamus is a hub of multiple functional networks and

370 receives afferent information from the spinal cord and then arrays it up to cortical regions [74–
371 76]. Specifically, the mediodorsal nucleus (MD) of the thalamus is relevant to nociceptive
372 inputs [77] and projects to the frontal cortex, such as the ACC and the aINS [78,79]. The
373 thalamus is also important in descending pain modulation [22,78], but understanding its
374 computational function remains difficult. Our modeling approach could solve this problem, not
375 only in the vision system, but in a variety of sensory modalities including pain, the thalamus
376 may regulate the influence of sensory input to determine to what extent a predicted latent state
377 encoded in the brain has to be corrected. In fact, the thalamus has two types of relay neurons,
378 core cells and matrix cells [80]; thus, it is natural to think that the MD of the thalamus controls
379 the influence of ascending nociceptive signals while relaying them up to the cortex.

380 In this paper, we considered the structure of the computational model that can produce
381 OA and OH. Highlighting the physiological anatomy, we proposed the neural implementation of
382 the model, especially connectivity between pain-related regions. As previous studies have
383 indicated [4–6], the pain system in the brain is so widely distributed that it is hard to understand
384 the functions of each region. Here, we adopted a constructive approach and considered the roles
385 of such regions in the framework of a Kalman filter model (Fig. 7). The structure of cortico-
386 brainstem connectivity was formulated as a measurement (*H*) matrix, and that of cortical
387 connectivity was formulated as the system (*A*) matrix, in which we assumed that the PAG
388 represents the prediction of pain intensity $\hat{y}$, which consisted of the latent state variables $\hat{x}_1$ and
389 $\hat{x}_2$ represented in the aINS and the ACC, respectively. In this scenario, $\hat{x}_1$ served as an integral
390 over time while $\hat{x}_2$ served as a derivative of stimulus change. The uncertainties of these state
391 variables shaped Kalman gain and altered the extent of OA. Previous computational modeling of
392 pain perception has strongly suggested a basic physiological anatomy. For example, a dual-state
393 adaptation model explained well the dynamics of habituation and sensitization, indicating distinct
394 neural systems of peripheral nerves and central nerves [81]. Thus, although our results do not

necessarily determine the whole structure of pain-related neural connectivity, they do provide insight into the computational understanding of neuroanatomy relevant to tonic pain processing.

# Methods

*The brain formulates an internal, generative model of causes of pain.*

We suppose that the brain represents an internal model of how various factors in the environment generate sensory signals processed by peripheral nerves. In this framework, the nociceptive stimulus intensity $y^{(k)}$ is also supposed to be generated from the integration of hidden causes of pain, described by the state vector $\mathbf{x}^{(k)}$:

$$y^{(k)} = H\mathbf{x}^{(k)} + \omega_y{}^{(k)}, \quad \omega_y{}^{(k)} \sim N(0, \sigma_y^2),$$

where $H$ is called a measurement matrix that characterizes how latent variables generate the stimulus intensity and $\omega_y$ is biological noise that has zero mean and $\sigma_y^2$ variance. The brain also supposes that according to the nature of painful events, causes of pain are continuous over time with a dynamical property, i.e., the cause at time $k+1$ is correlated with the cause at time $k$. This is mathematically defined by the state transition model:

$$\mathbf{x}^{(k+1)} = A\mathbf{x}^{(k)} + \boldsymbol{\varepsilon}^{(k)}, \quad \boldsymbol{\varepsilon} \sim N(0, \Omega_\varepsilon),$$

where $A$ is a transition matrix and $\Omega_\varepsilon$ is a covariance matrix of $\mathbf{x}$ representing a transition noise. Influenced by noise $\boldsymbol{\varepsilon}^{(k)}$, the cause of pain described by the state vector $\mathbf{x}^{(k)}$ determines the next-step cause of pain $\mathbf{x}^{(k+1)}$.

*Kalman filter theory*

Having such an internal model of tonic pain perception, the task for the brain is to estimate the values of the latent variables from the observed nociceptive stimulus intensity. We define $\hat{\mathbf{x}}^{(k|k-1)}$ as a state prediction at time $k$ given its estimate at time $k-1$, $\hat{\mathbf{x}}^{(k-1|k-1)}$. In a general framework of our modeling, we suppose that the state variable $\mathbf{x}$ is embedded in the environment and the prediction and estimation of this state variable $\hat{\mathbf{x}}$ are represented in the

brain. According to Kalman filter theory [33], the state prediction and the covariance matrix prediction are as follows, respectively:

$$\hat{\mathbf{x}}^{(k|k-1)} = A\hat{\mathbf{x}}^{(k-1|k-1)}, \qquad (1)$$

$$P^{(k|k-1)} = AP^{(k-1|k-1)}A^{\mathrm{T}} + \Omega_{\varepsilon}.$$

Then, the prediction of measurement is as follows:

$$\hat{y}^{(k)} = H\hat{\mathbf{x}}^{(k|k-1)}.$$

Then, the prediction error of the stimulus intensity is defined as $y^{(k)} - \hat{y}^{(k)}$. Thus, the optimal estimate of the state at time $k$, $\hat{\mathbf{x}}^{(k|k)}$, is computed from the predicted latent state, $\hat{\mathbf{x}}^{(k|k-1)}$ by the weighted prediction error as follows:

$$\hat{\mathbf{x}}^{(k|k)} = \hat{\mathbf{x}}^{(k|k-1)} + K^{(k)}(y^{(k)} - \hat{y}^{(k)}), \qquad (2)$$

where $K^{(k)}$ is a Kalman gain, which is a matrix reflecting the precision of state prediction and measurement noise as follows:

$$K^{(k)} = P^{(k|k-1)}H^{T}(\Omega_{\omega} + HP^{(k|k-1)}H^{T})^{-1}.$$

The Kalman gain also updates the covariance matrix:

$$P^{(k|k)} = (I - K^{(k)}H)P^{(k|k-1)}.$$

In summary, the state is predicted by Eqn.1 and is then integrated with the measurement by Eqn.2 to obtain the corrected state estimate. In this way, the tonic pain perception is modeled in the predictive coding framework, which assumes the prediction term of hidden causes of pain and the corrective term given by prediction error.

*Single-state vs. Two-state model*

In the single-state model, we defined the latent state as a scalar, $\mathbf{x}^{(k)} = x^{(k)}$. Then, the variance of transition noise is $\Omega_{\varepsilon} = \sigma_{\varepsilon}^2$ and the variance of measurement noise is $\Omega_{\omega} = \sigma_{\omega}^2$. We used the following parameters as $x^{(1)} = 0$, $\sigma_{\omega}^2 = 1$ after confirming that the simulation results in terms of OA/OH phenomena that were not sensitive to these parameter values. Here, we set the

transition matrix $A = 1$ and the measurement matrix $H = 1$ to examine in a simple way whether the single-state model could replicate OA and OH.

In the two-state models, we defined the latent state as a 2D vector, $\mathbf{x}^{(k)} = [x_1^{(k)} \quad x_2^{(k)}]^{\boldsymbol{T}}$. Then, the $2 \times 2$ covariance matrix of transition noise $\Omega_\varepsilon = \begin{bmatrix} \sigma_1^2 & \sigma_1\sigma_2 \\ \sigma_1\sigma_2 & \sigma_2^2 \end{bmatrix}$ while the variance of measurement noise was $\Omega_\omega = \sigma_\omega^2 = 1$ in the same way as the single-state model. Also, the initial values of the state variables were zero, $x_1^{(1)} = x_2^{(1)} = 0$. We defined the measurement matrix $H$ as $H = [b_1 \quad b_2]$ and the $2 \times 2$ transition matrix $A$ was defined as $A = \begin{bmatrix} a_{11} & a_{12} \\ a_{21} & a_{22} \end{bmatrix}$. To manipulate the $H$ matrix, there should be two possibilities. The first possibility is that two latent variables contribute to measurement estimation equivalently, whereas the other possibility is that only one variable estimates measurement. Thus, we specified here two model families, depending on the structure of the $H$ matrix, $[1 \quad 1]$ or $[1 \quad 0]$. Then, we designed conceivable components of the $A$ matrix in each model family. In the model family 1 ($H = [1 \quad 1]$), we tested the $A$ matrix of three different structures as below:

$$A_{NInt} = \begin{bmatrix} 1 & 0 \\ 0 & 1 \end{bmatrix},\ A_{UInt} = \begin{bmatrix} 1 & 1 \\ 0 & 1 \end{bmatrix},\ A_{BInt} = \begin{bmatrix} 1 & 1 \\ 1 & 1 \end{bmatrix}.$$

In the model family 2 ($H = [1 \quad 0]$), we also tested the same three structures:

$$A_{IUInt} = \begin{bmatrix} 1 & 0 \\ 1 & 1 \end{bmatrix},\ A_{UInt} = \begin{bmatrix} 1 & 1 \\ 0 & 1 \end{bmatrix},\ A_{BInt} = \begin{bmatrix} 1 & 1 \\ 1 & 1 \end{bmatrix}.$$

We ensured that, in all these $A$ matrices, the two components $a_{11}$ and $a_{22}$ were always set to 1, not zero. This is because these cells determine how each variable predicts its next value from the previous estimate, while $a_{12}$ and $a_{21}$ determine a way of predictive interaction between the variables. Such structural simplicity is helpful to examine only interactions between the variables.

We used the variance parameter of transition noise as $\sigma_\varepsilon^2 = 0.1$ in the single-state model and as $\sigma_1^2 = \sigma_2^2 = 0.1$, not correlated, $\sigma_1\sigma_2 = 0$ in the two-state models. For further investigation of this parameter in the two-state models, we manipulated $\sigma_1^2 = \sigma_2^2 = 0.1$, 0.03, 0.01, or 0.005.

*Pain intensity*

The relationship between the perceived intensity of the thermal stimulus and the presented temperature can be approximated by a linear function for a certain stimulus range [24,82]. Thus, let us define $y^{(k)}$ as the simple linear function of temperature $T^{(k)}$ above the pain threshold as follows:

$$y^{(k)} = T^{(k)} - threshold$$

This approximation is based on previous modeling [83,84], and here $threshold$ was set to 44°C based on the literature[83,84]. We adopted the pain rating scale of the previous study on OA [18–20], which defined non-painful perception as rating 0 and perceived pain intensity as more than 0 (the imaginable pain intensity as 10). Thus, $y^{(k)}$ represents the perceived pain intensity in this rating scale. That is why we plotted the simulation results of "Pain intensity" as more than zero by setting it to zero if less than zero.

## Acknowledgments

This work was supported by KAKENHI (grant number 19H05729)

## Author Contributions

Conceptualization, RI and JI; methodology, RI and JI; investigation, RI and JI; formal analysis, RI; writing – original draft, RI and JI; writing – review & editing, R. and JI.

# References


1. Mano H, Seymour B. Pain: a distributed brain information network? PLoS biology. 2015. p. e1002037.

2. Geuter S, Reynolds Losin EA, Roy M, Atlas, Lauren Y, Schmidt L, Krishnan A, et al. Multiple Brain Networks Mediating Stimulus–Pain Relationships in Humans. Cereb Cortex. 2020;30: 4204–4219.

3. Bushnell MC, Ceko M, Low LA. Cognitive and emotional control of pain and its disruption in chronic pain. Nat Rev Neurosci. 2013;14: 502–511.

4. Talbot JD, Marrett S, Evans AC, Meyer E, Bushnell MC, Duncan GH. Multiple representations of pain in human cerebral cortex. Science. 1991;251: 1355–1358.

5. Wager TD, Atlas LY, Lindquist MA, Roy M, Woo C-W, Kross E. An fMRI-based neurologic signature of physical pain. N Engl J Med. 2013;368: 1388–1397.

6. Woo C-W, Schmidt L, Krishnan A, Jepma M, Roy M, Lindquist MA, et al. Quantifying cerebral contributions to pain beyond nociception. Nat Commun. 2017;8: 14211.

7. Price DD. Psychological and neural mechanisms of the affective dimension of pain. Science. 2000;288: 1769–1772.

8. Schweinhardt P, Bushnell MC. Pain imaging in health and disease--how far have we come? J Clin Invest. 2010;120: 3788–3797.

9. Davis KD, Flor H, Greely HT, Iannetti GD, Mackey S, Ploner M, et al. Brain imaging tests for chronic pain: medical, legal and ethical issues and recommendations. Nat Rev Neurol. 2017;13: 624–638.

10. Geisler WS, Kersten D. Illusions, perception and Bayes. Nature neuroscience. 2002. pp. 508–510.

11. Friston K. The history of the future of the Bayesian brain. Neuroimage. 2012;62: 1230–1233.

12. Knill DC, Pouget A. The Bayesian brain: the role of uncertainty in neural coding and computation. Trends Neurosci. 2004;27: 712–719.

13. Ernst MO, Banks MS. Humans integrate visual and haptic information in a statistically optimal fashion. Nature. 2002;415: 429–433.

14. Ernst MO. Learning to integrate arbitrary signals from vision and touch. J Vis. 2007;7: 7.1-14.

15. Anchisi D, Zanon M. A Bayesian perspective on sensory and cognitive integration in pain perception and placebo analgesia. PLoS One. 2015;10: e0117270.

16. Büchel C, Geuter S, Sprenger C, Eippert F. Placebo analgesia: a predictive coding perspective. Neuron. 2014;81: 1223–1239.

17. Tabor A, Thacker MA, Moseley GL, Körding KP. Pain: A Statistical Account. PLoS Comput Biol. 2017;13: e1005142.

18. Atlas LY, Bolger N, Lindquist MA, Wager TD. Brain mediators of predictive cue effects on

526 perceived pain. J Neurosci. 2010;30: 12964–12977.

527 19. Yoshida W, Seymour B, Koltzenburg M, Dolan RJ. Uncertainty increases pain: evidence for
528 a novel mechanism of pain modulation involving the periaqueductal gray. J Neurosci.
529 2013;33: 5638–5646.

530 20. Fields HL. How expectations influence pain. Pain. 2018;159: S3–S10.

531 21. Grill JD, Coghill RC. Transient analgesia evoked by noxious stimulus offset. J Neurophysiol.
532 2002;87: 2205–2208.

533 22. Yelle MD, Oshiro Y, Kraft RA, Coghill RC. Temporal filtering of nociceptive information
534 by dynamic activation of endogenous pain modulatory systems. J Neurosci. 2009;29: 10264–
535 10271.

536 23. Yelle MD, Rogers JM, Coghill RC. Offset analgesia: a temporal contrast mechanism for
537 nociceptive information. Pain. 2008;134: 174–186.

538 24. Mørch CD, Frahm KS, Coghill RC, Arendt-Nielsen L, Andersen OK. Distinct temporal
539 filtering mechanisms are engaged during dynamic increases and decreases of noxious
540 stimulus intensity. Pain. 2015;156: 1906–1912.

541 25. Alter BJ, Aung MS, Strigo IA, Fields HL. Onset hyperalgesia and offset analgesia: Transient
542 increases or decreases of noxious thermal stimulus intensity robustly modulate subsequent
543 perceived pain intensity. PLoS One. 2020;15: e0231124.

544 26. Fust J, Lalouni M, Vadenmark Lundqvist V, Wärnberg E, Jensen KB. Offset analgesia and
545 onset hyperalgesia with different stimulus ranges. PAIN Reports. 2021;6: e914.

546 27. Niesters M, Hoitsma E, Sarton E, Aarts L, Dahan A. Offset analgesia in neuropathic pain
547 patients and effect of treatment with morphine and ketamine. Anesthesiology. 2011;115:
548 1063–1071.

549 28. Niesters M, Proto PL, Aarts L, Sarton EY, Drewes AM, Dahan A. Tapentadol potentiates
550 descending pain inhibition in chronic pain patients with diabetic polyneuropathy. Br J
551 Anaesth. 2014;113: 148–156.

552 29. Oudejans LCJ, Smit JM, van Velzen M, Dahan A, Niesters M. The influence of offset
553 analgesia on the onset and offset of pain in patients with fibromyalgia. Pain. 2015;156: 2521–
554 2527.

555 30. Suzan E, Treister R, Pud D, Haddad M, Eisenberg E. The effect of hydromorphone therapy
556 on psychophysical measurements of the descending inhibitory pain systems in patients with
557 chronic radicular pain. Pain Med. 2015;16: 168–175.

558 31. Kobinata H, Ikeda E, Zhang S, Li T, Makita K, Kurata J. Disrupted offset analgesia
559 distinguishes patients with chronic pain from healthy controls. Pain. 2017;158: 1951–1959.

560 32. Szikszay TM, Adamczyk WM, Luedtke K. The Magnitude of Offset Analgesia as a Measure
561 of Endogenous Pain Modulation in Healthy Participants and Patients With Chronic Pain: A
562 Systematic Review and Meta-Analysis. Clin J Pain. 2019;35: 189–204.

563 33. Shulman J, Zurakowski D, Keysor J, Jervis K, Sethna NF. Offset analgesia identifies
564 impaired endogenous pain modulation in pediatric chronic pain disorders. Pain. 2020;161:
565 2852–2859.

34. Zhang S, Li T, Kobinata H, Ikeda E, Ota T, Kurata J. Attenuation of offset analgesia is associated with suppression of descending pain modulatory and reward systems in patients with chronic pain. Mol Pain. 2018;14: 1744806918767512.

35. Hermans L, Calders P, Van Oosterwijck J, Verschelde E, Bertel E, Meeus M. An Overview of Offset Analgesia and the Comparison with Conditioned Pain Modulation: A Systematic Literature Review. Pain Physician. 2016;19: 307–326.

36. Kalman RE. A new approach to linear filtering and prediction problems. J Basic Eng. 1960;82: 35–45.

37. Song Y, Yao M, Kemprecos H, Byrne A, Xiao Z, Zhang Q, et al. Predictive coding models for pain perception. J Comput Neurosci. 2021;49: 107–127.

38. Friston K. Hierarchical models in the brain. PLoS Comput Biol. 2008;4: e1000211.

39. Friston K. The free-energy principle: a unified brain theory? Nat Rev Neurosci. 2010;11: 127–138.

40. Barron HC, Auksztulewicz R, Friston K. Prediction and memory: A predictive coding account. Prog Neurobiol. 2020;192: 101821.

41. Idei H, Ohata W, Yamashita Y, Ogata T, Tani J. Sensory attenuation develops as a result of sensorimotor experience. arXiv [q-bio.NC]. 2021. Available: http://arxiv.org/abs/2111.02666

42. Cassidy CM, Balsam PD, Weinstein JJ, Rosengard RJ, Slifstein M, Daw ND, et al. A Perceptual Inference Mechanism for Hallucinations Linked to Striatal Dopamine. Curr Biol. 2018;28: 503-514.e4.

43. Sterzer P, Adams RA, Fletcher P, Frith C, Lawrie SM, Muckli L, et al. The Predictive Coding Account of Psychosis. Biol Psychiatry. 2018;84: 634–643.

44. Friston KJ, Stephan KE, Montague R, Dolan RJ. Computational psychiatry: the brain as a phantastic organ. Lancet Psychiatry. 2014;1: 148–158.

45. Oliva V, Gregory R, Davies W-E, Harrison L, Moran R, Pickering AE, et al. Parallel cortical-brainstem pathways to attentional analgesia. Neuroimage. 2021;226: 117548.

46. Grahl A, Onat S, Büchel C. The periaqueductal gray and Bayesian integration in placebo analgesia. Elife. 2018;7. doi:10.7554/eLife.32930

47. Geuter S, Eippert F, Hindi Attar C, Büchel C. Cortical and subcortical responses to high and low effective placebo treatments. Neuroimage. 2013;67: 227–236.

48. Wiech K, Eippert F, Vandekerckhove J, Zaman J, Placek K, Tuerlinckx F, et al. Cortico-brainstem mechanisms of biased perceptual decision-making in the context of pain. J Pain. 2021. doi:10.1016/j.jpain.2021.11.006

49. Heinricher MM, Tavares I, Leith JL, Lumb BM. Descending control of nociception: Specificity, recruitment and plasticity. Brain Res Rev. 2009;60: 214–225.

50. Derbyshire SWG, Osborn J. Offset analgesia is mediated by activation in the region of the periaqueductal grey and rostral ventromedial medulla. Neuroimage. 2009;47: 1002–1006.

51. Eippert F, Bingel U, Schoell ED, Yacubian J, Klinger R, Lorenz J, et al. Activation of the

opioidergic descending pain control system underlies placebo analgesia. Neuron. 2009;63: 533–543.

52. Tinnermann A, Geuter S, Sprenger C, Finsterbusch J, Büchel C. Interactions between brain and spinal cord mediate value effects in nocebo hyperalgesia. Science. 2017;358: 105–108.

53. Ploner M, Lee MC, Wiech K, Bingel U, Tracey I. Prestimulus functional connectivity determines pain perception in humans. Proc Natl Acad Sci U S A. 2010;107: 355–360.

54. Geuter S, Boll S, Eippert F, Büchel C. Functional dissociation of stimulus intensity encoding and predictive coding of pain in the insula. Elife. 2017;6. doi:10.7554/eLife.24770

55. Eippert F, Finsterbusch J, Bingel U, Büchel C. Direct evidence for spinal cord involvement in placebo analgesia. Science. 2009;326: 404.

56. Geuter S, Büchel C. Facilitation of pain in the human spinal cord by nocebo treatment. J Neurosci. 2013;33: 13784–13790.

57. Seymour B. Pain: A Precision Signal for Reinforcement Learning and Control. Neuron. 2019;101: 1029–1041.

58. Seymour B, Mancini F. Hierarchical models of pain: Inference, information-seeking, and adaptive control. Neuroimage. 2020;222: 117212.

59. Villemure C, Bushnell MC. Mood influences supraspinal pain processing separately from attention. J Neurosci. 2009;29: 705–715.

60. Brooks JCW, Davies W-E, Pickering AE. Resolving the Brainstem Contributions to Attentional Analgesia. J Neurosci. 2017;37: 2279–2291.

61. Sawamoto N, Honda M, Okada T, Hanakawa T, Kanda M, Fukuyama H, et al. Expectation of pain enhances responses to nonpainful somatosensory stimulation in the anterior cingulate cortex and parietal operculum/posterior insula: an event-related functional magnetic resonance imaging study. J Neurosci. 2000;20: 7438–7445.

62. Koyama T, McHaffie JG, Laurienti PJ, Coghill RC. The subjective experience of pain: where expectations become reality. Proc Natl Acad Sci U S A. 2005;102: 12950–12955.

63. Wiech K, Kalisch R, Weiskopf N, Pleger B, Stephan KE, Dolan RJ. Anterolateral prefrontal cortex mediates the analgesic effect of expected and perceived control over pain. J Neurosci. 2006;26: 11501–11509.

64. Salomons TV, Johnstone T, Backonja M-M, Davidson RJ. Perceived controllability modulates the neural response to pain. J Neurosci. 2004;24: 7199–7203.

65. Wiech K, Lin C-S, Brodersen KH, Bingel U, Ploner M, Tracey I. Anterior insula integrates information about salience into perceptual decisions about pain. J Neurosci. 2010;30: 16324–16331.

66. Sharvit G, Corradi-Dell'Acqua C, Vuilleumier P. Modality-specific effects of aversive expectancy in the anterior insula and medial prefrontal cortex. Pain. 2018;159: 1529–1542.

67. Wiech K, Jbabdi S, Lin CS, Andersson J, Tracey I. Differential structural and resting state connectivity between insular subdivisions and other pain-related brain regions. Pain. 2014;155: 2047–2055.

644 68. Hong J-Y, Kilpatrick LA, Labus JS, Gupta A, Katibian D, Ashe-McNalley C, et al. Sex and
645 disease-related alterations of anterior insula functional connectivity in chronic abdominal
646 pain. J Neurosci. 2014;34: 14252–14259.

647 69. Peltz E, Seifert F, DeCol R, Dörfler A, Schwab S, Maihöfner C. Functional connectivity of
648 the human insular cortex during noxious and innocuous thermal stimulation. Neuroimage.
649 2011;54: 1324–1335.

650 70. Taylor KS, Seminowicz DA, Davis KD. Two systems of resting state connectivity between
651 the insula and cingulate cortex. Hum Brain Mapp. 2009;30: 2731–2745.

652 71. Baliki MN, Geha PY, Apkarian AV. Parsing pain perception between nociceptive
653 representation and magnitude estimation. J Neurophysiol. 2009;101: 875–887.

654 72. Kanai R, Komura Y, Shipp S, Friston K. Cerebral hierarchies: predictive processing,
655 precision and the pulvinar. Philos Trans R Soc Lond B Biol Sci. 2015;370.
656 doi:10.1098/rstb.2014.0169

657 73. Fischer J, Whitney D. Attention gates visual coding in the human pulvinar. Nat Commun.
658 2012;3: 1051.

659 74. Hwang K, Shine JM, Bruss J, Tranel D, Boes A. Neuropsychological evidence of multi-
660 domain network hubs in the human thalamus. Elife. 2021;10: e69480.

661 75. Guest JM, Bast A, Narayanan RT, Oberlaender M. Thalamus gates active dendritic
662 computations in cortex during sensory processing. bioRxiv. 2021. p. 2021.10.21.465325.
663 doi:10.1101/2021.10.21.465325

664 76. Constantinople CM, Bruno RM. Deep cortical layers are activated directly by thalamus.
665 Science. 2013;340: 1591–1594.

666 77. Lindstedt F, Johansson B, Martinsen S, Kosek E, Fransson P, Ingvar M. Evidence for
667 thalamic involvement in the thermal grill illusion: an FMRI study. PLoS One. 2011;6:
668 e27075.

669 78. Delevich K, Tucciarone J, Huang ZJ, Li B. The mediodorsal thalamus drives feedforward
670 inhibition in the anterior cingulate cortex via parvalbumin interneurons. J Neurosci. 2015;35:
671 5743–5753.

672 79. Meda KS, Patel T, Braz JM, Malik R, Turner ML, Seifikar H, et al. Microcircuit Mechanisms
673 through which Mediodorsal Thalamic Input to Anterior Cingulate Cortex Exacerbates Pain-
674 Related Aversion. Neuron. 2019;102: 944-959.e3.

675 80. Jones EG. Viewpoint: the core and matrix of thalamic organization. Neuroscience. 1998;85:
676 331–345.

677 81. Jepma M, Jones M, Wager TD. The dynamics of pain: evidence for simultaneous site-
678 specific habituation and site-nonspecific sensitization in thermal pain. J Pain. 2014;15: 734–
679 746.

680 82. Beck B, Gnanasampanthan S, Iannetti GD, Haggard P. No temporal contrast enhancement
681 of simple decreases in noxious heat. J Neurophysiol. 2019;121: 1778–1786.

682 83. Cecchi GA, Huang L, Hashmi JA, Baliki M, Centeno MV, Rish I, et al. Predictive dynamics
683 of human pain perception. PLoS Comput Biol. 2012;8: e1002719.

84. Petre B, Tetreault P, Mathur VA, Schurgin MW, Chiao JY, Huang L, et al. A central mechanism enhances pain perception of noxious thermal stimulus changes. Sci Rep. 2017;7: 3894.

# Figures

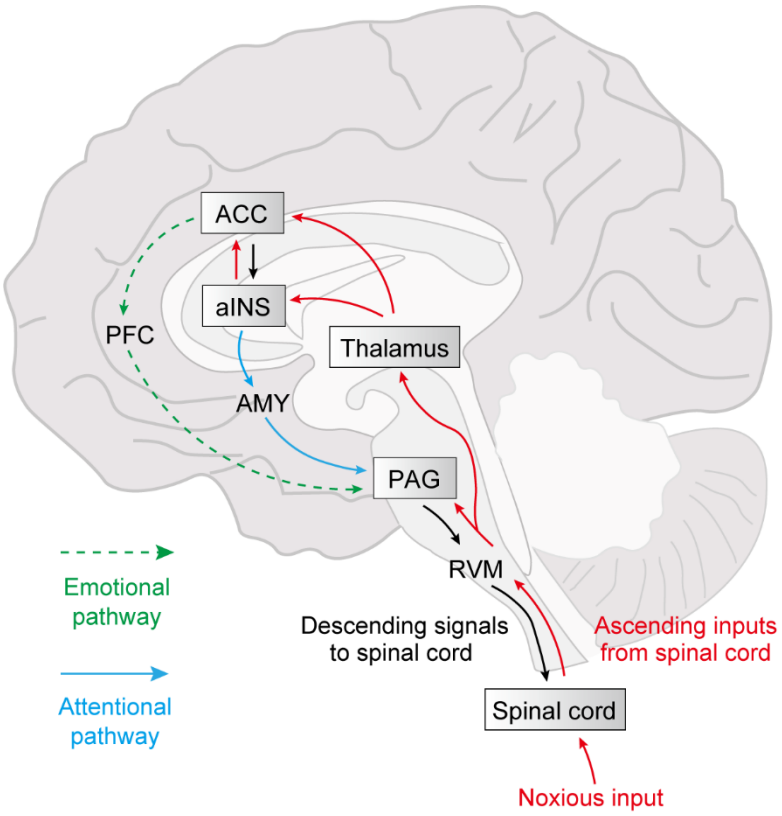


Fig.1

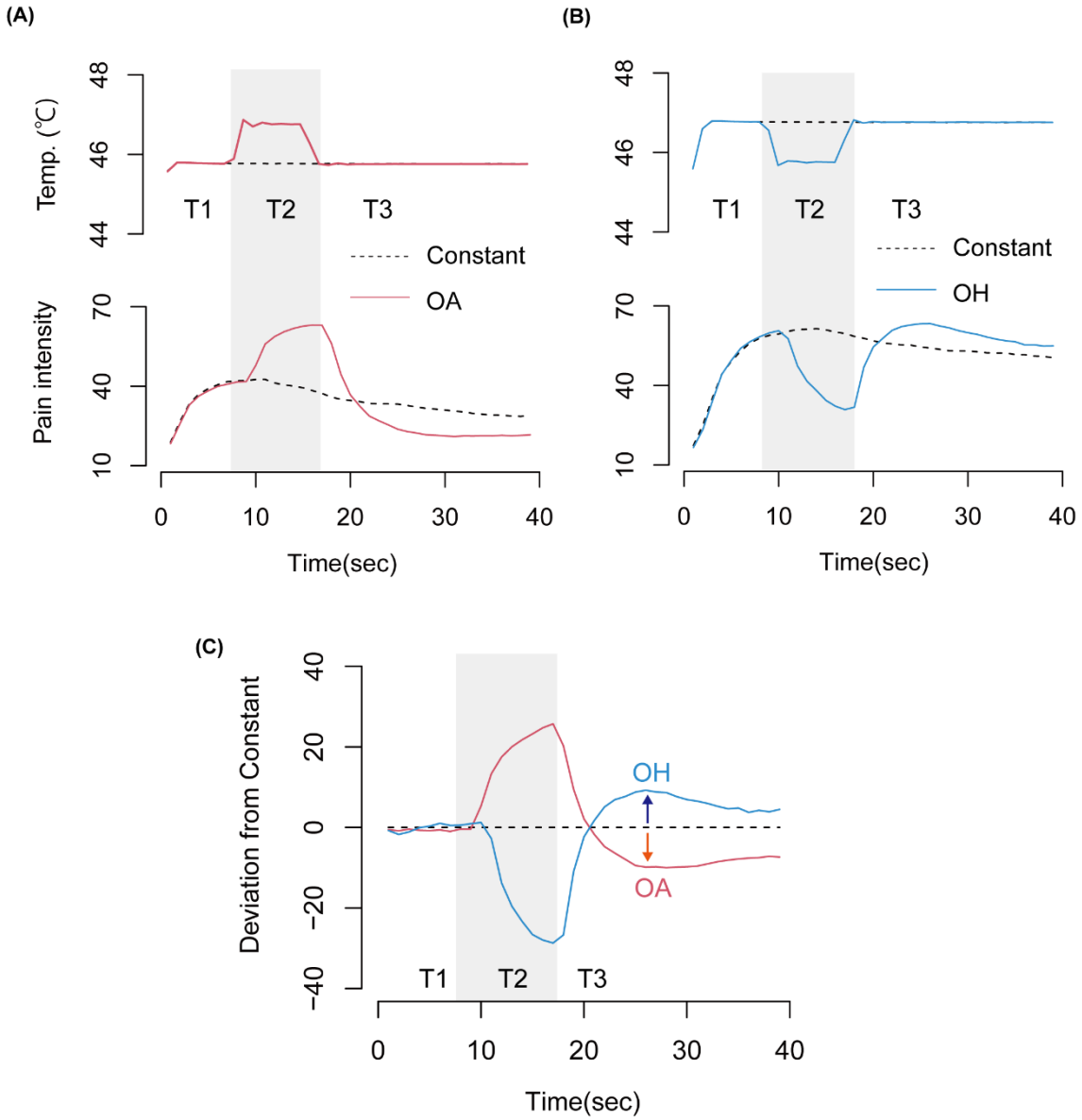


694

695 Fig.2

696

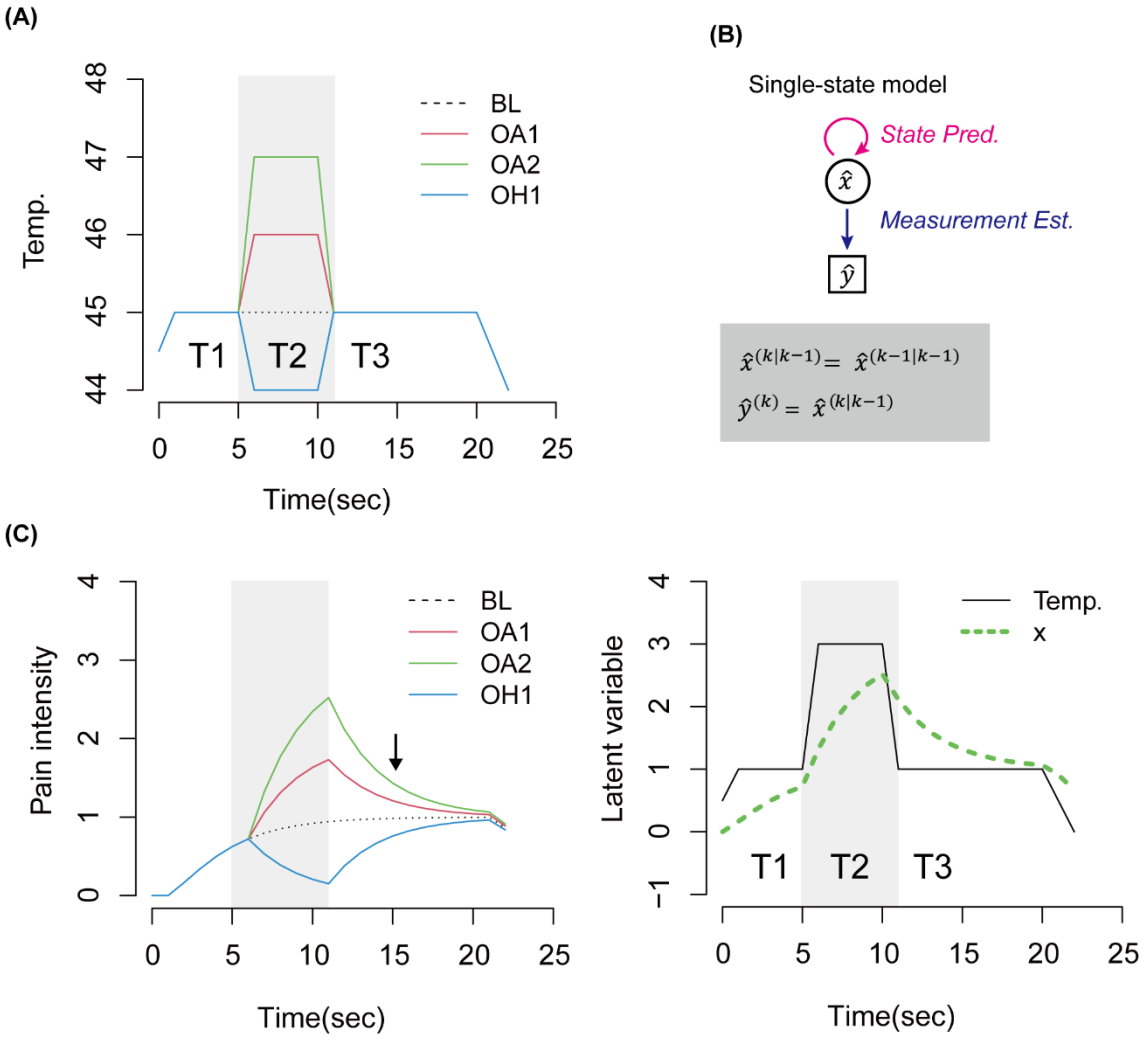


Fig. 3

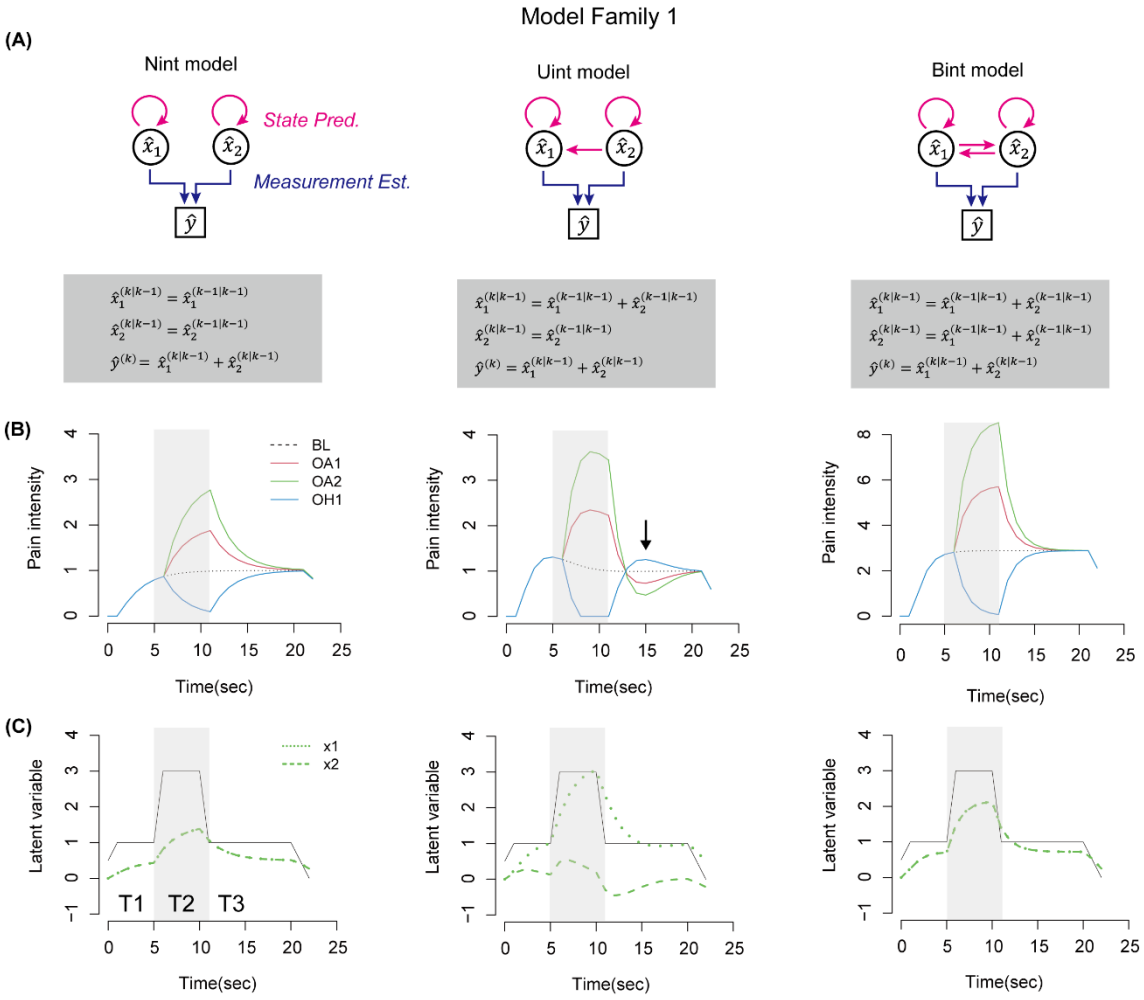


Fig. 4

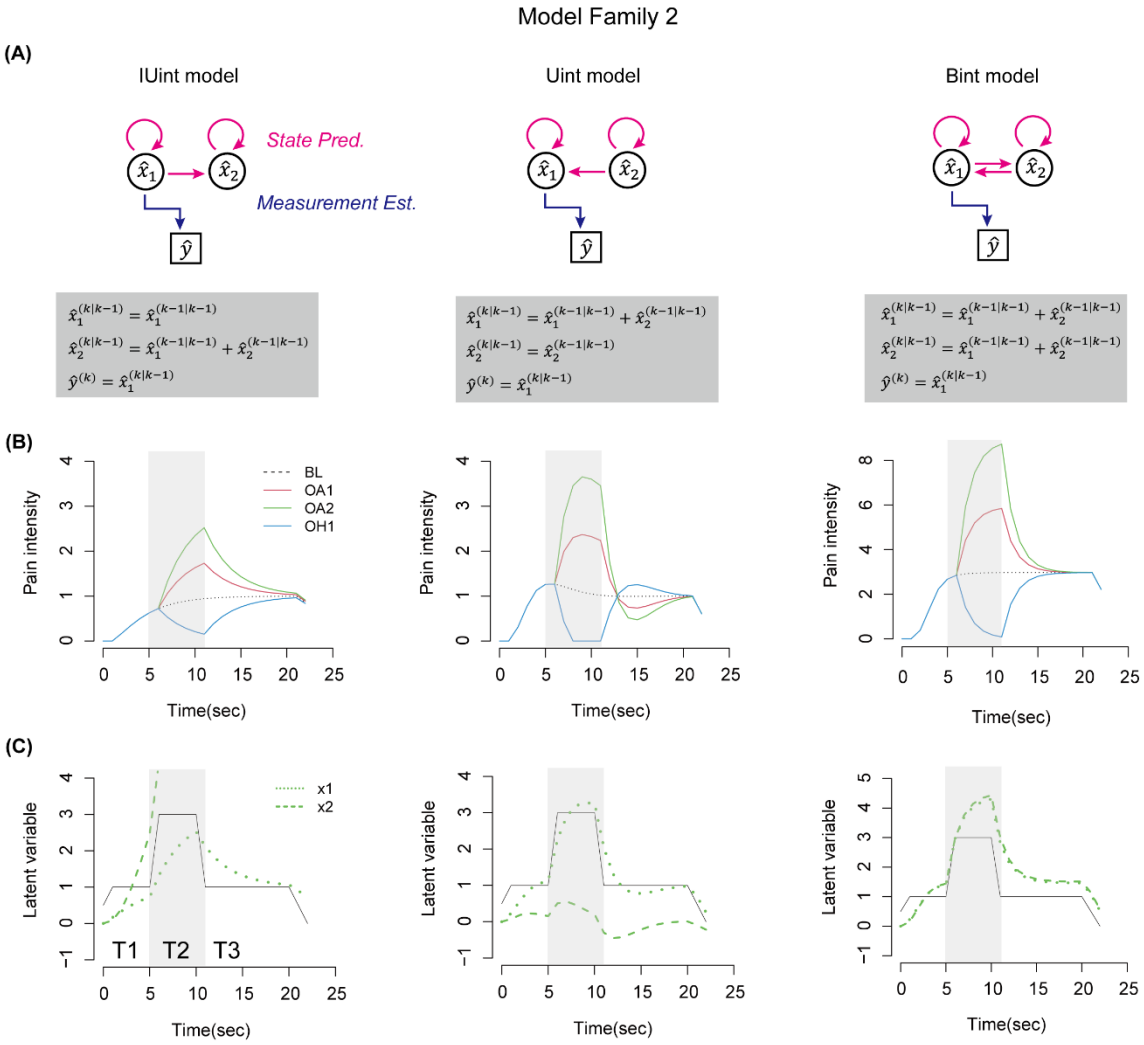


Fig. 5

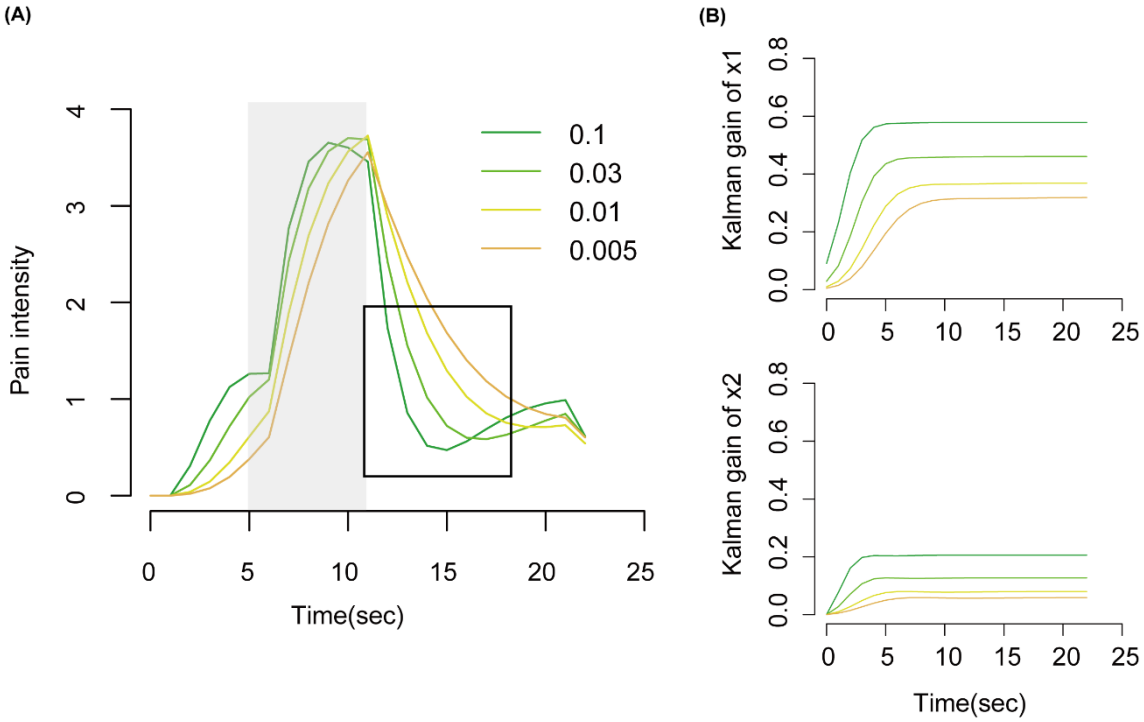


706

707 Fig. 6

708

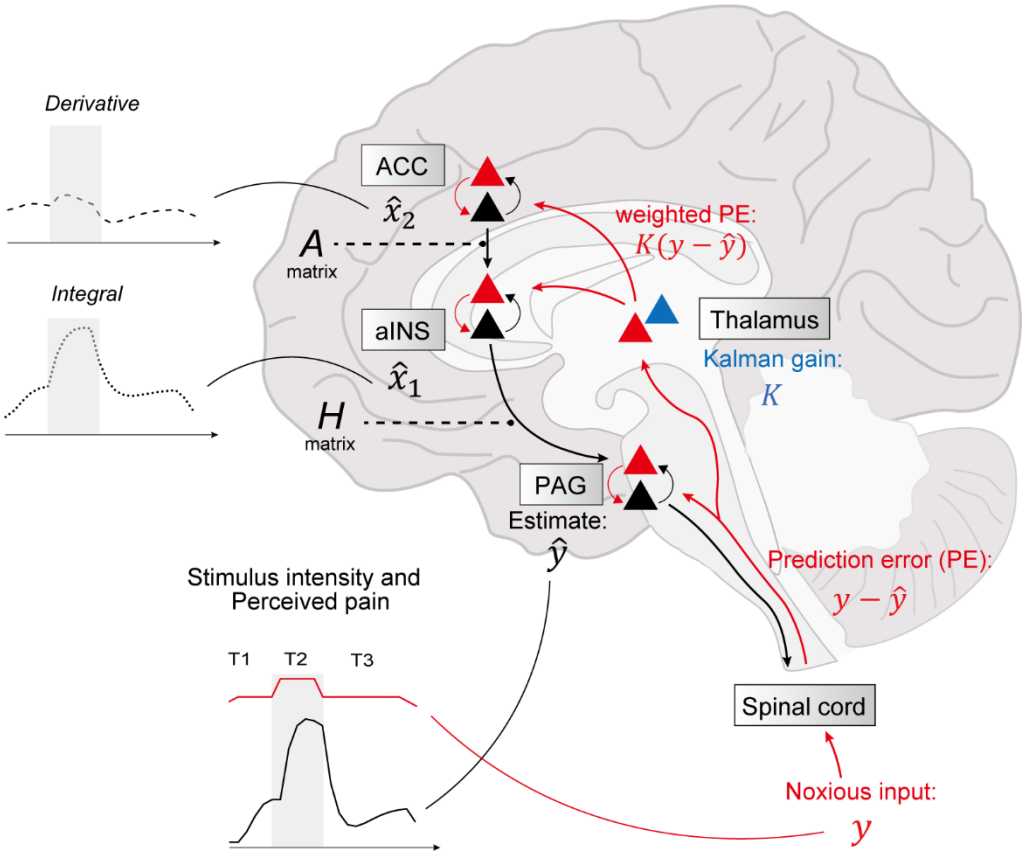


Fig. 7